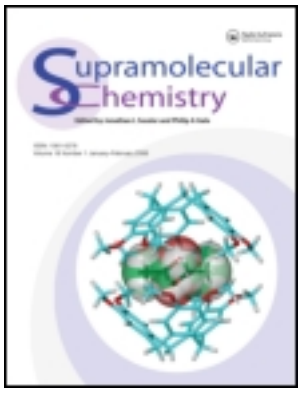

Supramolecular Chemistry
Publication details, including instructions for authors and subscription information:
http://www.tandfonline.com/loi/gsch20

Supramolecular self-assembly of protoporphyrin IX amphiphiles into worm-like and particular aggregates

Sheshanath V. Bhosale [a], Mohan B. Kalyankar [b], Sidhanath V. Bhosale [b], Sudhakar G. Patil [a], Cecilia H. Lalander [a], Steven J. Langford [a] & Santosh V. Nalage [b]

[a] School of Chemistry, Monash University, Clayton, 3800, Australia

[b] Department of Organic Chemistry, North Maharashtra University, Jalgaon, 425 001, India

Available online: 13 Apr 2011

To cite this article: Sheshanath V. Bhosale, Mohan B. Kalyankar, Sidhanath V. Bhosale, Sudhakar G. Patil, Cecilia H. Lalander, Steven J. Langford & Santosh V. Nalage (2011): Supramolecular self-assembly of protoporphyrin IX amphiphiles into worm-like and particular aggregates, Supramolecular Chemistry, 23:03-04, 263-268

To link to this article: http://dx.doi.org/10.1080/10610278.2010.523115

Supramolecular Chemistry
Vol. 23, Nos. 3–4, March–April 2011, 263–268

Supramolecular self-assembly of protoporphyrin IX amphiphiles into worm-like and particular aggregates

Sheshanath V. Bhosale[a]*, Mohan B. Kalyankar[b], Sidhanath V. Bhosale[b]*, Sudhakar G. Patil[a], Cecilia H. Lalander[a], Steven J. Langford[a] and Santosh V. Nalage[b]

[a]*School of Chemistry, Monash University, Clayton 3800, Australia;* [b]*Department of Organic Chemistry, North Maharashtra University, Jalgaon 425 001, India*

(*Received 1 June 2010; final version received 8 September 2010*)

A protoporphyrin IX amphiphile bearing hydrophobic–hydrophilic functional regions was synthesised by coupling protoporphyrin IX with methoxytriethylene glycol using (3-(dimethylamino)propyl)ethyl carbodiimide hydrochloride/1-hydroxybenzotriazole followed by a double-cross metathesis with 1-undecene using second-generation Grubb's catalyst. The self-assembling behaviour of the amphiphile in varying concentration of $CHCl_3$/MeOH was investigated, with well-defined nanostructures described as worm-like fibrils and particular aggregates being formed in 1:1 and 1:9 v/v of MeOH/$CHCl_3$, respectively.

Keywords: protoporphyrin IX; self-assembly; nanoaggregates; AFM

Introduction

Protoporphyrin IX is the iron-free form of haem, one of the most common natural sources of porphyrin. Its antipodal, peripheral functionalisation can be exploited through differing chemistries to fine-tune the physical properties of the core porphyrin for exploiting self-assembly phenomena (*1*). Protoporphyrin amphiphiles consisting of apolar rigid northern and polar mobile southern regions have been used to prepare *pseudo*-1D and -3D nanostructures (*2–8*). The difference in self-assembly is attributed to small changes in the hydrophilic edge of the protoporphyrin IX (*9*, *10*). Despite some examples, the controlled self-assembly of naturally occurring protoporphyrin derivatives has not yet been extensively studied. For example, while vesicles, vesicular tubules, micellar fibres and few other controlled structures have been fabricated, the 1D self-assembly of protoporphyrin molecules remains challenging, though useful in studying energy and electron transfer processes (*9–14*). More recently, a functionalised porphyrin bearing triethylene glycol (TEG) (hydrophilic) at one end and alkyl chains (hydrophobic) on the other end was shown to be self-assembled into a variety of structures in a solvent-dependent manner (*15*). Herein, we report a synthesis and self-assembly of protoporphyrin amphiphile **1** into nanoscale particles and worm-like structure with varying concentration of methanol in chloroform (Figure 1) as a means of expanding our recent results around the *solvo-control* of nanostructured materials (*16*, *17*).

Results and discussion

Amphiphile **1** consists of a rigid, apolar hydrophobic northern part, comprising long alkyl chains in positions 3 and 8 of the porphyrin macrocycle, and a flexible hydrophilic southern part in the form of methoxyTEG chains. The differing phobicity of each chain along with their length and the presence of a rigid, flat core typically supports other self-assembled processes that lead to soft materials or liquid crystallinity over crystallisation.

Compound **1** was prepared in two steps (Scheme 1). The first involves coupling of protoporphyrin IX with methoxyTEG amine in the presence of (3-(dimethylamino)propyl)ethyl carbodiimide hydrochloride (EDCI)/1-hydroxybenzotriazole (HOBt) in dry DMF at room temperature. As a result compound **2** was formed in 95% yield. Cross-metathesis of **2** with 1-undecene using second-generation Grubb's catalyst in dry THF under argon atmosphere gives the bis-alkene as essentially the *E*-isomer in 84% yield (Scheme 1).

UV–vis and fluorescence spectroscopy

Protoporphyrin derivative **1** is very soluble in chloroform and presents a spectrum that is expected based on the porphyrinic core (Figure 2(a)). Salient features include an intense Soret band at 408 nm ($\varepsilon = 1.65 \times 10^5\,M^{-1}\,cm^{-1}$), together with four weaker Q-bands at 506, 542, 577 and 630 nm. Figure 2(a) also shows the absorption spectra of **1** in various ratios of methanol and chloroform. As the ratio

*Corresponding authors. Email: sheshanath.bhosale@monash.edu; sidhanath2003@yahoo.co.in

ISSN 1061-0278 print/ISSN 1029-0478 online

DOI: 10.1080/10610278.2010.523115
http://www.informaworld.com

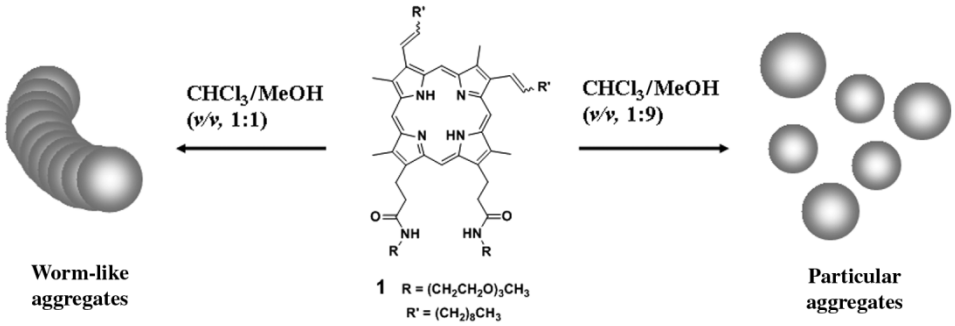

Figure 1. Proposed model of self-assembly of **1** into particular and worm-like aggregates in different concentration of chloroform and methanol.

of methanol to chloroform increases, aggregation is evidenced as a result of the reduction in peak intensity and loss of fine structure within the bands along with a small blue shift of the absorption maxima (*16*). The fluorescence emission of **1** shows the two bands at 616 and 688 nm in neat $CHCl_3$ (Figure 2(b)) (*17*). Upon addition of methanol (0, 25, 50 and 100% v/v), the fluorescence emission is quenched to varying degrees, which is attributed to the self-assembly of **1** into aggregates that effect the electronic structure. The fact that the fluorescence emission is

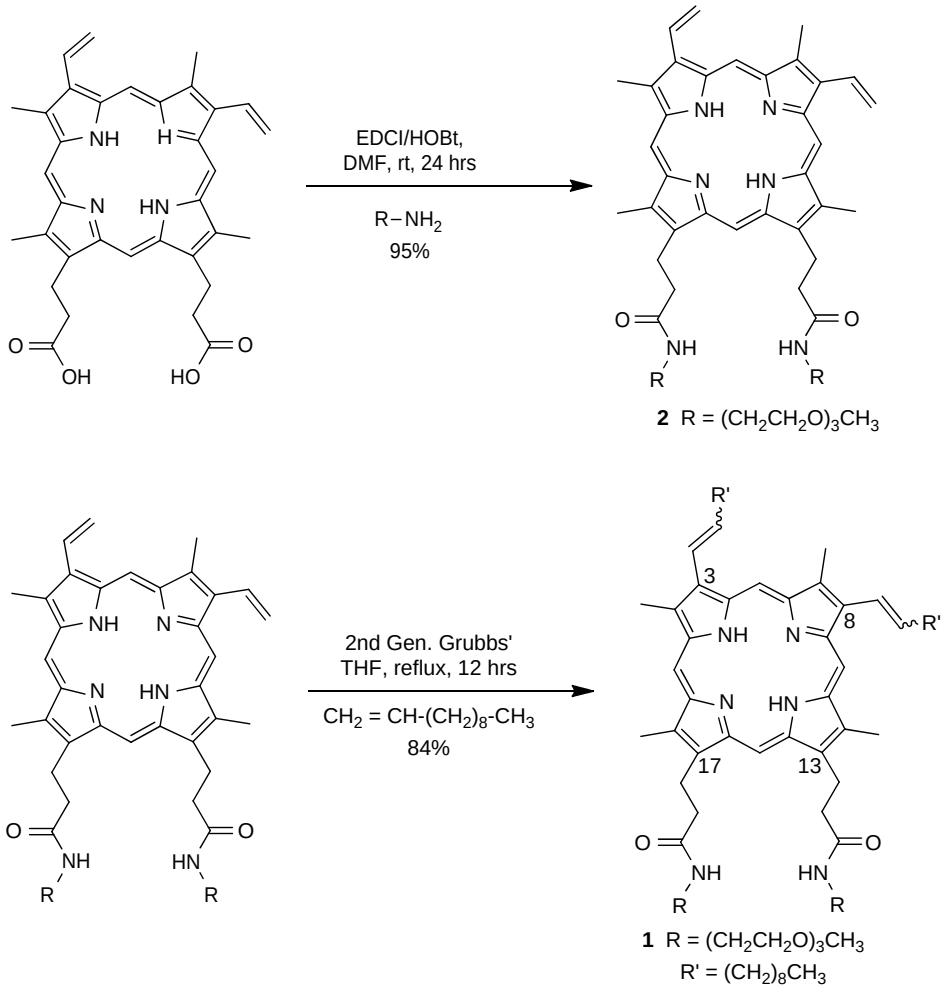

Scheme 1. Synthesis of target protoporphyrin amphiphilic derivative **1**.

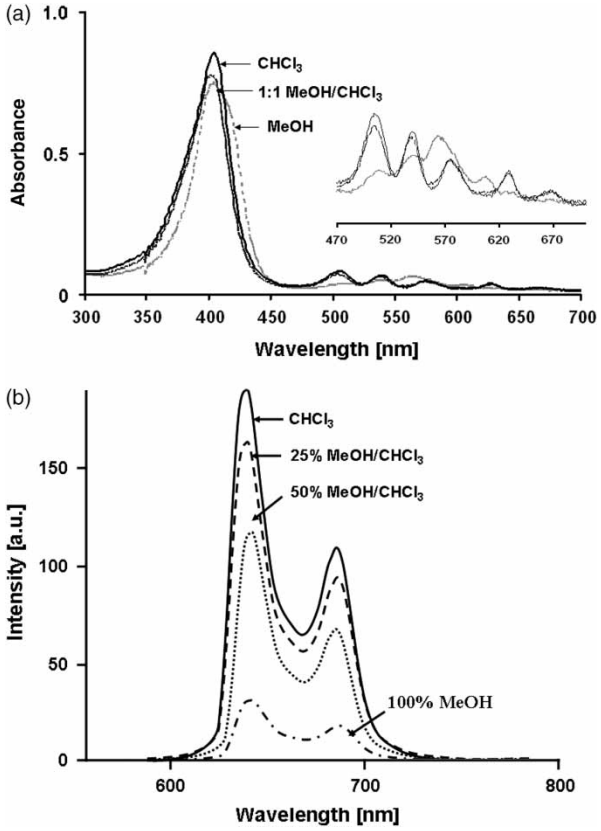

Figure 2. Spectroscopic characterisation of **1**: (a) UV–vis absorption and (b) emission spectroscopy in varying concentration of $CHCl_3$/MeOH.

slightly red shifted in increasing methanol concentration lends some support to *J*-type aggregation of **1** similar to that experienced by tetraphenylporphyrin (*18–20*). This type of aggregation may be directed by the peripheral alkyl and oligoethylene groups with a co-operativity that leads to the final aggregate type. Interestingly, no specific change was observed for **1** in $CHCl_3$/cyclohexane mixes indicating a *solvo-controlled* self-assembly process, as hydrophilic–hydrophobic balance is important for aggregation of **1** (*20–22*).

AFM, transmission electron microscopy and dynamic light scattering measurements

Atomic force microscopy (AFM) images of **1** ([**1**] = 0.5 μM) in $CHCl_3$/methanol (1:1 and 1:9, v/v) were taken by spin-coating solutions of **1** on plasma-cleaned silica (111) wafers and examined in the tapping mode at ambient conditions. AFM images of **1** from $CHCl_3$/methanol (1:1, v/v) showed worm-like fibril supramolecular self-assemblies (Figure 3), among irregular aggregated nanostructures. The lengths of the fibrils exceed 50–100 nm, and the widths are approximately 2–4 nm. The ratio of the diameter and height of the nanostructures formed by **1** also suggest a flattening upon being transferred from solution to silicon surface (Figure 3(d)).

Dynamic light scattering (DLS) experiments on **1** ([**1**] = 1×10^{-4} M) in $CHCl_3$/MeOH (v/v, 1:9) support the presence of particular aggregates in solution. The hydrodynamic radius (R_H) of the vesicles derived from the characteristic line width was obtained from the DLS data by the CONTIN analysis method (*13*) which show that the R_H values have scarcely any angular dependence, supporting the formation of spherical aggregates. In most cases, the polydispersity index (PDI) is higher than normal values making it difficult to analyse the data; however, in certain instances, a sharp peak with an average radius of about 40 nm is observed with a PDI of 0.10 (Figure 4(a)). No aggregates of **1** in $CHCl_3$ solution were observed by DLS. AFM images of **1** in methanol/$CHCl_3$ (9:1, v/v) show well-defined nanoparticles of approximately 50–60 nm diameter.

Transmission electron microscopy (TEM) images (Figure 5) were prepared of **1** ([**1**] = 0.5 μM) in $CHCl_3$/methanol (1:9, v/v) when deposited on a carbon grid. Clearly evident are larger spherical aggregates as well as an ultrafine fibrous network. The diameter obtained from AFM also corresponds to the thicker nanoparticles observed by TEM.

Experimental

Material

Protoporphyrin IX, DMF, 1-undecene, Grubb's second-generation catalyst, 3-EDCI, HOBt, chloroform, methanol, cyclohexane and dichloromethane were purchased from Sigma-Aldrich (Sydney, Australia) and used without purification. UV–vis absorption spectra were recorded on a PerkinElmer (Waltham, MA, USA) Lambda 40 p spectrometer. ^{1}H NMR and ^{13}C NMR spectra were recorded on a Bruker DRX spectrometer using chloroform-*d* as solvent and residual solvent as an internal standard. The solvents for spectroscopic studies were of spectroscopic grade and used as received. A stock solution of **1** was prepared in chloroform and self-assembled samples were prepared by diluting stock solution of **1** in $CHCl_3$/MeOH mixed solvents. The sample solutions were kept at room temperature for few hours before TEM and AFM measurement.

Synthesis of protoporphyrin IX amphiphile 1

Synthesis of compound 2

Protoporphyrin IX (100 mg, 0.17 mmol) and HOBt (71 mg, 0.53 mmol) were combined in DMF (10 ml) under argon atmosphere. The resulting solution was cooled to 0°C, stirred for 40 min, then EDCI (100 mg, 0.53 mmol) was added and the solution was stirred for a further 60 min at 0°C. MethoxyTEG amine (130 mg, 0.53 mmol) in DMF

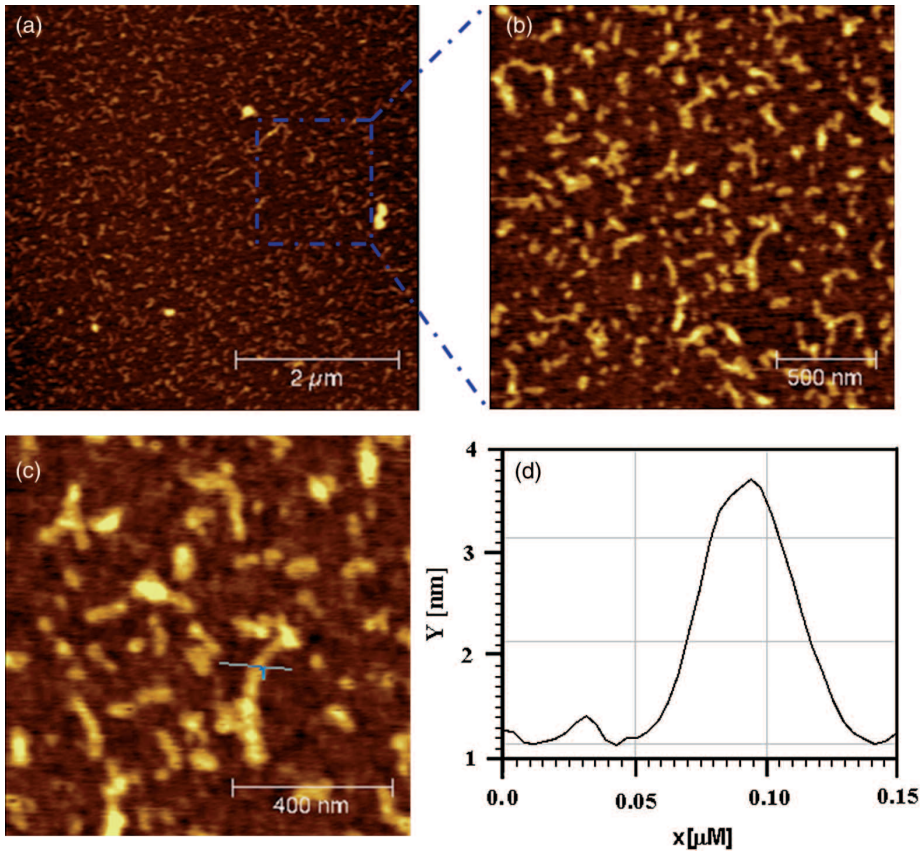

Figure 3. AFM images of **1** in $CHCl_3$/MeOH (1:1, v/v) spin-cast onto silica wafers showing (a) worm-like fibrils, (b) a magnified image over a bundle marked in (a), (c) height image and (d) cross-section analysis magnified region from image.

(2 ml) was added at once and the resulting solution stirred for an additional 4 h at 0°C, then warmed to room temperature and left to stir for further 24 h. After this time, the reaction solvent (DMF) was removed by rotary evaporation under reduced pressure, and the gummy reaction mixture was eluted with dichloromethane (100 ml) and washed with aqueous 10% w/v $NaHCO_3$ solution (2 × 30 ml), 0.1 M HCl (20 ml), followed by water (20 ml) and brine (20 ml). The resultant organic solvent was dried over sodium sulphate, filtered and reduced *in vacuo*. The residue was purified by flash silica gel chromatography (SiO_2) by eluting first with chloroform followed by a 2% v/v methanol in chloroform solution to give **2** as dark violet crystalline material (82 mg, 95%). ^{1}H NMR ($CDCl_3$, 400 MHz) δ: −4.07 (br s, 2H), 2.21 (s, 12H), 2.4–2.6 (m, 8H), 3.03–3.52 (m, 20H), 3.56 (s, 6H), 4.23 (t, 4H, $J = 7.7$ Hz), 6.14 (d, 2H, $J = 7.6$ Hz), 6.89 (d, 2H, $J = 7.8$ Hz), 8.17 (m, 2H), 9.97 (m, 1H), 10.00 (m, 3H). ^{13}C NMR ($CDCl_3$, 125 MHz): δ 173.3, 142.1, 137.5, 137.4, 135.9, 129.8, 120.0, 97.7, 95.4, 96.7, 71.6, 71.5, 69.8, 69.7, 69.5, 69.3, 69.2, 58.8, 36.8, 21.7, 12.8, 12.7, 11.8, 11.7. UV–vis ($CHCl_3$) λ_{max} (log ε) 403 (5.16), 503 (4.03), 538 (3.94), 6573 (3.61), 627 (3.36) nm. LS-MS *m/z* 853.3 $(M + H)^+$, 875.2 $(M + Na)^+$. HR-MS-ESI *m/z* calcd for $C_{48}H_{64}N_6O_8$ 852.4786, found 852.4785 $(M)^+$.

*Protoporphyrin IX amphiphile **1***

Compound **2** (50 mg, 0.06 mmol) and 1-undecene (45 mg, 0.2 mmol) were combined in THF (10 ml) under an argon atmosphere. Then a solution of Grubb's catalyst (6 mg, 0.01 mmol) in THF (2 ml) was added via syringe to the reaction mixture. The reaction mixture was refluxed under an argon atmosphere for 12 h, after which the reaction solvent (THF) was removed by rotary evaporation under reduced pressure. The residue was eluted with dichloromethane (100 ml) and washed with a 10% w/v $NaHCO_3$ solution (2 × 30 ml), 0.1 M HCl (20 ml), followed by water (20 ml), and the organic solvent was dried over sodium sulphate, filtered and concentrated to dryness. The residue was purified by flash chromatography (SiO_2), eluting first with dichloromethane followed by a 4% v/v methanol in dichloromethane solution to yield **1** as a dark violet crystalline material (55 mg, 84%). ^{1}H NMR ($CDCl_3$, 400 MHz) δ: ^{1}H NMR ($CDCl_3$, 400 MHz): δ −4.07 (br s, 2H), 0.5–0.7 (m, 6H), 1.2–1.5 (m, 24H), 1.7 (m, 4H), 1.3

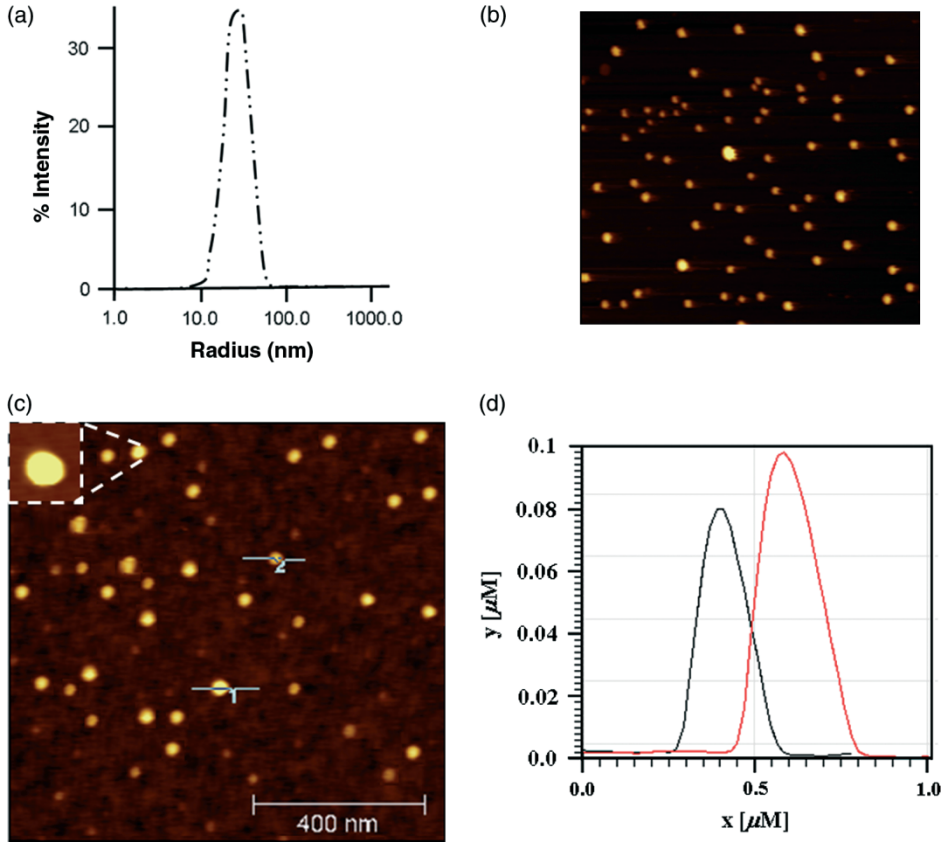

Figure 4. Self-assembly of **1** in $CHCl_3$/MeOH (1:9, v/v): (a) DLS, (b) AFM images of spin-cast silica wafers, (c) height image showing a magnified particle and (d) cross-section analysis of magnified region from image 'c'.

(m, 4H), 2.21 (s, 12H), 2.4–2.6 (m, 8H), 3.03–3.52 (m, 20H), 3.56 (s, 6H), 4.23 (t, 4H, $J = 7.7$ Hz), 6.14 (d, 2H, $J = 7.6$ Hz), 6.89 (d, 2H, $J = 7.8$ Hz), 9.97 (m, 1H), 10.00 (m, 3H). ^{13}C NMR ($CDCl_3$, 125 MHz) δ: 173.3, 142.1, 137.5, 137.4, 135.9, 129.8, 120.0, 97.7, 95.4, 96.7, 71.6, 71.5, 69.8, 69.7, 69.5, 69.3, 69.2, 58.8, 36.8, 33.9, 31.9, 30.1, 29.8, 29.7, 29.5, 29.4, 22.7, 21.7, 14.1, 12.8, 12.7, 11.8, 11.7. HR-MS-ESI *m/z* calcd for $C_{67}H_{102}N_6O_8$: 1104.7603, found 1104.7602 $(M)^+$.

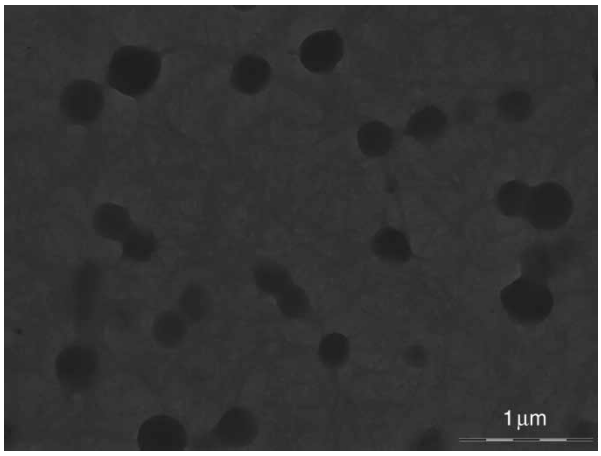

Figure 5. TEM image of **1** from $CHCl_3$/MeOH (1:9, v/v) deposited on holey carbon film showing the particular and fibril aggregates. The TEM sample was prepared by drop-casting of **1** in $CHCl_3$/MeOH (1:9, v/v) solution.

UV–vis spectroscopy

Solutions of protoporphyrin **1** in $CHCl_3$/MeOH (1.5 mM as the final concentration) were used to obtain spectra. The UV–vis measurements were recorded at room temperature using a PerkinElmer Lambda 40 p spectrophotometer equipped with a 0.1 cm path length cuvette.

AFM and TEM studies

TEM images were taken on a Philips model CM-200, operating voltage 200 kV, with a resolution of 2.4 Å. TEM studies of **1** were carried out using a 10 μl of the solution of **1** from $CHCl_3$/MeOH (1:9, v/v) on carbon-coated copper grid (400-mesh) by slow evaporation to dryness in vacuum at room temperature. AFM images were recorded using a 5500 AFM from Agilent Technologies (Santa Clara, CA, USA). Micromach ultrasharp probes with silica wafers coating for enhanced reflectivity (NSC15/AIBS), with

a typical resonance frequency of 325 kHz and a force constant of 40 N/m, were used for imaging. Samples of **1** were prepared by spin coating the freshly prepared solution (1×10^{-4} M in $CHCl_3$/MeOH or $CHCl_3$/cyclohexane) onto silica coating at 2000 rpm.

DLS study

These measurements were performed using a Malvern Nano-ZS zetasizer (Malvern Instruments Ltd, Worcestershire, UK). The Nano-ZS employs non-invasive backscatter optical technology and measures real-time changes in intensity of scattered light as a result of particles undergoing Brownian motion. The sample was illuminated by a 633 nm helium–neon laser and a maximum output power of 100 mW was used as light source and measurements were performed at an angle of 55°. The size distribution of the particles was calculated from the diffusion coefficient of the particles according to Stokes–Einstein equation. The average radius and the PDI of the samples were calculated by the software using CONTIN analysis (*13*). Freshly prepared samples of **1** with a concentration of 1×10^{-4} M in methanol were used for DLS measurements. DLS measurements show the existence of aggregates with $R_H = 40$ nm in coexistence with several larger sized species. The relative amount of the two species depends on concentration and time, but it was not possible to remove the larger particles by filtration or by any other common method.

Conclusion

In summary, we have demonstrated the assembly of a protoporphyrin derivative **1** bearing two different side chain types antipodally displaced. The nature of the self-assembly is solvent dependent and concentration dependent by taking advantage of the solvophobicity of the side chains in chloroform–methanol mixes. We are also currently working on the metallated versions of **1** using zinc and tin(IV) complexes in order to gain more insight into the electric conductivities of cation and anion π-radicals (*23*).

Acknowledgements

Sid. V.B. would like to thank CSIR, New Delhi, India, for financial assistance [Project No. 01 (2283)/08/EMR-II] and Shesh. V.B. and S.J.L. gratefully acknowledge the Australian Research Council for support under the Discovery Programme (DP0878756 and DP0878220). We also thank B. Patro and P. Varghese (IIT Bombay) for TEM measurements.

References

(1) Liu, X.; Sternberg, E.; Dolphin, D. *Chem. Commun.* **2004**, 852–853.
(2) Lehn, J.-M. *Science* **2002**, *295*, 2400–2403.
(3) Charvet, R.; Jiang, D.-L.; Aida, T. *Chem. Commun.* **2004**, 2664–2665.
(4) Tsuchida, E.; Komatsu, T.; Arai, K.; Yamada, K.; Nishide, H.; Fuhrhop, J.H. *Langmuir* **1995**, *11*, 1877–1884.
(5) Tsuchida, E.; Komatsu, T.; Arai, K.; Yamada, K.; Nishide, H.; Böttcher, C.; Fuhrhop, J.H. *J. Chem. Soc. Chem. Commun.* **1995**, 1063–1064.
(6) Komatsu, T.; Tsuchida, E.; Böttcher, C.; Donner, D.; Messerschmidt, C.; Siggel, U.; Stocker, W.; Rabe, J.P.; Fuhrhop, J.-H. *J. Am. Chem. Soc.* **1997**, *119*, 11660–11665.
(7) Fuhrhop, J.H. In *Stereochemistry of Lipid Micelles and Vesicles Which Survive Drying*; Texter, J., Ed.; M. Dekker Inc.: New York, 2001; Vol. 100, p 715.
(8) Drain, C.M.; Batteas, J.D.; Flynn, G.W.; Milic, T.; Chi, N.; Yablon, D.G.; Sommers, H. *Proc. Natl Acad. Sci. USA* **2002**, *99*, 6498.
(9) White, W.I. In *The Porphyrins*; Dolphin, D., Ed.; Academic Press: New York, 1978; Vol. 5, Chapter 7.
(10) Suslick, K.S.; Chen, C.-T.; Meredith, G.R.; Cheng, L.-T. *J. Am. Chem. Soc.* **1992**, *114*, 6928–6930.
(11) Endisch, C.; Bottcher, C.; Fuhrhop, J.-H. *J. Am. Chem. Soc.* **1995**, *117*, 8273–8274.
(12) Komatsu, T.; Yamada, K.; Tsuchida, E.; Siggel, U.; Bottcher, C.; Fuhrhop, J.-H. *Langmuir* **1996**, *12*, 6242–6249.
(13) Scolaro, L.M.; Castriciano, M.; Romeo, A.; Patane, S.; Cefali, E.; Allegrini, M. *J. Phys. Chem. B* **2002**, *106*, 2453–2459.
(14) Fuhrhop, J.-H.; Demoulin, C.; Böttcher, C.; Koning, J.; Siggel, U. *J. Am. Chem. Soc.* **1992**, *114*, 4159–4165.
(15) Oda, M.; Ishizuka, T.; Arai, S.; Takano, A.; Jiang, D. *Tetrahedron Lett.* **2009**, *50*, 7137–7140.
(16) Bhosale, S.V.; Jani, C.H.; Lalander, C.H.; Langford, S.J. *Chem. Commun.* **2010**, *46*, 973–975.
(17) Okada, S.; Segawa, H. *J. Am. Chem. Soc.* **2003**, *125*, 2792–2796.
(18) Takeuchi, M.; Tanaka, S.; Shinkai, S. *Chem. Commun.* **2005**, 5539–5541.
(19) Kitahama, Y.; Kimura, Y.; Takazawa, K. *Langmuir* **2006**, *22*, 7600–7604.
(20) Luca, G.; Romeo, A.; Scolaro, L. *J. Phys. Chem. B* **2006**, *110*, 7309–7315.
(21) Komatsu, T.; Moritake, M.; Tsuchida, E. *Chem. Eur. J.* **2003**, *9*, 4626–4633.
(22) Okada, S.; Segawa, H. *J. Am. Chem. Soc.* **2003**, *125*, 2792–2796.
(23) Fuhrhop, J.-H.; Kadish, D.G.; Davis, D.G. *J. Am. Chem. Soc.* **1973**, *95*, 5140–5147.